Research & Design of Nuclear Engineering, **2**, 2026002 (2026)
© Y. Zhang. et al. 2026. Published by EDP Sciences
https://doi.org/10.1051/rdne/2026002

Available online at:
https://rdne.edpsciences.org/

REVIEW ARTICLE OPEN ACCESS

Recent progress on the separation of lanthanide/actinide elements from nuclear wastes

Yue Zhang[1,2,★], Xiangcheng Jin[1,★], Meng Wang[1], Kai Sun[1], Meng Ge[1,3], Shin-ichiro Noro[2,*], and Yi Liu[1,3,*]

[1] State Key Laboratory of Fine Chemicals, Frontiers Science Center for Smart Materials, School of Chemical Engineering, Dalian University of Technology, Dalian 116024, PR China
[2] Faculty of Environmental Earth Science, Hokkaido University, Sapporo 060-0810, Japan
[3] Dalian Key Laboratory of Membrane Materials and Membrane Processes, Dalian University of Technology, Dalian 116024, PR China

Received: 13 December 2025 / Accepted: 14 September 2026

Abstract. High-efficient separation of actinides (An) from chemically similar lanthanides (Ln) in high-level liquid waste (HLLW) is a paramount challenge towards sustainable nuclear energy through closed fuel cycles and radioactive waste minimization via partitioning and transmutation (P&T). This necessity stems from their nearly identical physicochemical properties, specifically closely comparable ionic radii and highly analogous coordination behavior. Solvent extraction, exemplified by industrial processes like PUREX (plutonium uranium recovery by extraction) and TALSPEAK (trivalent actinide-lanthanide separation by phosphorous reagent extraction from aqueous complexes), remains dominant due to high selectivity and operational maturity. However, it faces significant limitations, including organic waste generation, extractant degradation, and carbon footprint. Alternative technologies aim to overcome these drawbacks. Crystallization separation exploits oxidation-state differences, achieving ultra-high selectivity without organic solvents, but struggles with ligand acid stability and An separation. Adsorption separation utilizes functionalized solid-phase materials, offering environmental benefits and radiation resistance; however, it is hindered by slow kinetics in concentrated feeds. Membrane separation leverages size-sieving or complexation mechanisms, providing low mass transfer resistance and continuous operation potential, but requires complex pre-treatment or uncertain ligand modification. Future advancements require synergistic innovation across three interconnected fronts: (1) Molecular design of rigid, multidentate ligands incorporating soft N-donors and exploiting effects like Anomalous Aryl Strengthening (AAS) to enhance An/Ln selectivity and stability under extreme conditions; (2) Process innovation integrating green technologies (e.g., supercritical CO_2 extraction, biomimetic adsorbents) to eliminate secondary waste and developing multi-stage hybrid strategies to circumvent single-method limitations; (3) Engineering optimization focusing on enhancing mass transfer, simplifying fabrication, and implementing intelligent controls. Overcoming these challenges is crucial for developing efficient, environmentally benign, and industrially viable An/Ln separation technologies to underpin advanced nuclear fuel cycles.

Keywords: Actinide/lanthanide separation / Solvent extraction / Membrane separation / Crystallization separation / Adsorption separation / Spent nuclear fuel reprocessing.

1 Introduction

Nuclear energy, as a highly efficient and low-carbon energy source, has been widely deployed globally since the 1950s [1]. Its applications include nuclear power generation [2–6], radiology and cancer medicine [7] (Figs. 1a–1b). Furthermore, nuclear energy plays a role in the transformation of the global energy structure and the pursuit of carbon neutrality goals [2, 6, 8] (Fig. 1c–d). However, the large-scale utilization of nuclear energy is accompanied by the generation of high-level radioactive spent nuclear fuel (SNF) [4, 8–12] and the risk of environmental contamination following nuclear accidents [13]. Thus, the safe disposal and effective resource utilization of SNF pose severe challenges to the sustainable development of nuclear energy.

SNF contains over 95% underutilized uranium (U) and plutonium (Pu). Currently, most nations employ the

★These authors contributed equally to this work.
* e-mails: diligenliu@dlut.edu.cn (Yi Liu); noro@ees.hokudai.ac.jp (Shin-ichiro Noro)

This is an Open Access article distributed under the terms of the Creative Commons Attribution License (https://creativecommons.org/licenses/by/4.0), which permits unrestricted use, distribution, and reproduction in any medium, provided the original work is properly cited.

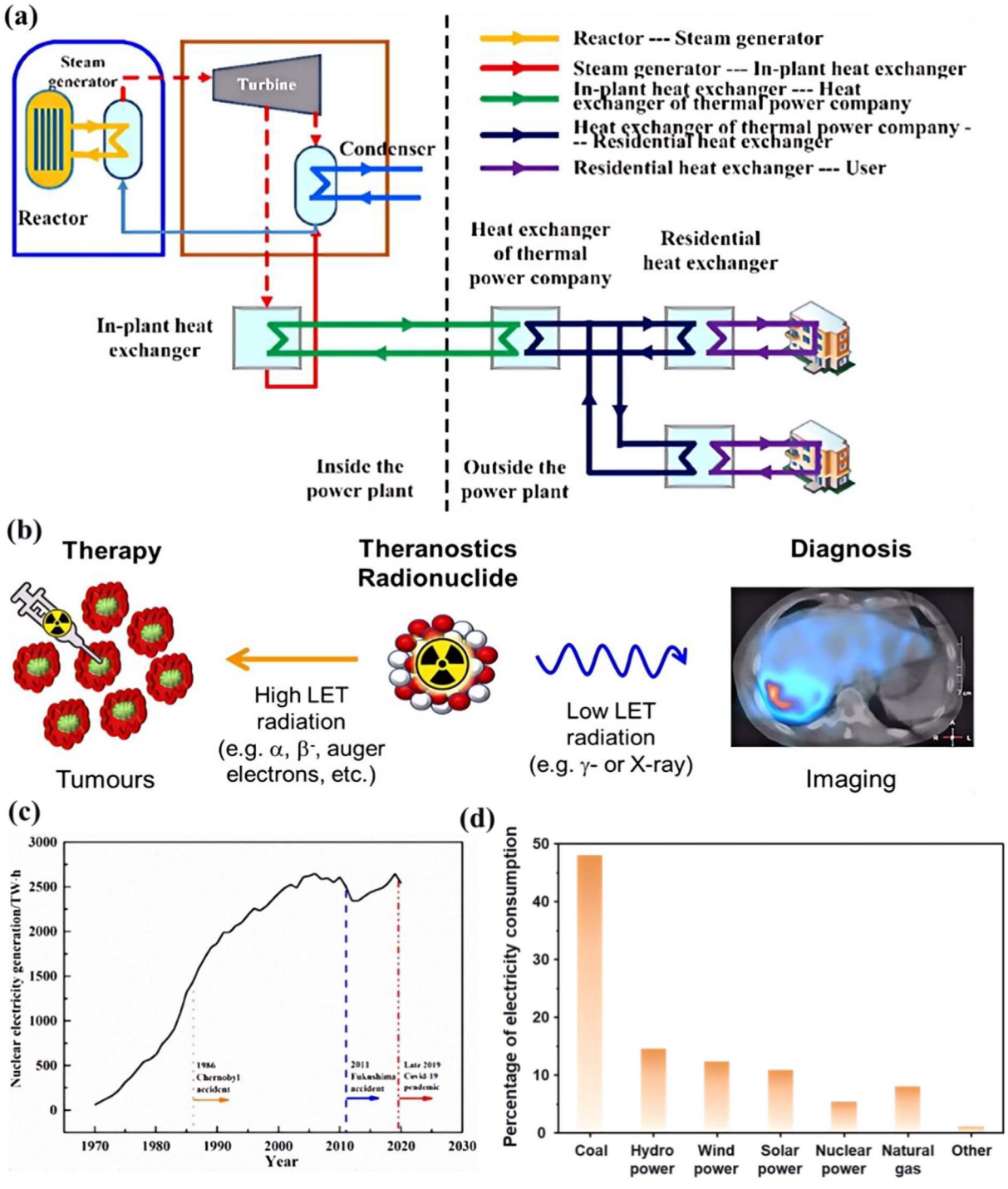


Fig. 1. (a) Nuclear energy in district heating; (b) nuclear energy in radiology and cancer medicine [14]; (c) annual nuclear electricity generation since the 1970s (IAEA, 2022a) [14, 15]; (d) the proportion of nuclear power in electricity consumption (IEA, Ember, EIA, national energy administration, 2026).

PUREX process, developed in the 1950s, to recover these elements [6, 12, 16–18]. The recovered materials are fabricated into Mixed Oxide (MOX) fuel for reuse in nuclear reactors [19]. However, this process generates approximately 1% of the SNF by mass as HLLW. This waste stream contains the primary determinants of long-term environmental risk: long-lived minor actinides (MAs) such as americium (Am), curium (Cm), and neptunium (Np), alongside significant quantities of fission products, predominantly Ln. MAs possess extremely high radiotoxicity and decay periods that span tens of thousands of years, making them the principal source of long-term thermal load and

radiotoxicity in geological repositories [2, 10, 12, 20, 21]. While the P&T strategy aims to convert MAs into short-lived or stable nuclides-significantly reducing the required isolation time to centuries and substantially mitigating repository burden and risk [6, 18, 22]-its core bottleneck lies in achieving the efficient separation of An from Ln [17, 23, 24].

Consequently, the separation of An and Ln is recognized as one of the foremost chemical challenges in the nuclear fuel cycle. This stems from their remarkable physicochemical similarities [3, 4, 6]: 1) Comparable Ionic Radii [12, 18, 22]: Influenced by the lanthanide contraction and actinide contraction effects, their ionic radii exhibit minimal differences (e.g., $r(Am^{3+}) = 1.115$ Å, $r(Eu^{3+}) = 1.087$ Å). 2) Similar Charge Density and Coordination Behavior [22, 25]: According to the Hard and Soft Acids and Bases (HSAB) theory, both An and Ln elements behave as hard Lewis acids, exhibiting a strong preference for coordination with oxygen-donor ligands. They form highly hydrated ions with large coordination numbers in aqueous solutions, which leads to nearly identical chemical behaviors.

This near-identical nature renders traditional separation methods-such as precipitation and conventional solvent extraction, largely inadequate. Crucially, Ln act as potent "neutron poisons" due to their significantly higher neutron capture cross-sections compared to MAs. Failure to achieve effective separation results in residual Ln severely blocking neutrons, drastically reducing MAs transmutation efficiency and potentially undermining the P&T strategy. Current industrial-scale separation technologies, such as the U.S. reference process TALSPEAK, are fundamentally based on the "soft–hard separation" principle. Specifically, compared to the localized and weakly bonding 4f orbitals of Ln, the 5f orbitals of An are more spatially extended and higher in energy. This results in significantly greater overlap between the wavefunctions of their electron clouds and ligand orbitals. When coordinating with "soft" donor atoms such as nitrogen or sulfur, the 5f orbitals of An can participate more substantially in the frontier molecular orbitals. As a consequence, An–N/S bonds exhibit stronger covalent character relative to Ln–N/S bonds. This subtle difference in covalency forms the electronic structural basis for their separation from Ln. The TALSPEAK process precisely leverages this nuanced distinction in covalent interaction by employing soft nitrogen/sulfur-containing donor ligands (e.g., 3,4,3-LI(1,2-HOPO), HOPO) to selectively chelate the more covalent An ions in the aqueous phase, while hard O-donor extractants (e.g., di-(2 ethylhexyl) phosphoric acid, HDEHP) in the organic phase selectively extract Ln [12]. However, significant limitations persist, including a narrow operational pH window (pH 3.5–4.0), the requirement for costly buffer systems, slow extraction kinetics, and overall complexity. Furthermore, solvent extraction itself suffers from inherent drawbacks: large equipment footprint, generation of difficult-to-treat organic radioactive mixed waste, and challenges in tolerating high radiation fields and extreme acidity. Therefore, the development of efficient, highly selective, environmentally benign, and engineering-feasible new technologies for An/Ln separation constitutes a critical scientific frontier. This advancement is essential for achieving radioactive waste minimization.

Several separation methods, including solvent extraction, membrane separation, countercurrent chromatography, crystallization, and adsorption, have been explored for An/Ln separation. Consequently, this review focuses on the research progress of solvent extraction, membrane separation, crystallization, and adsorption separation for actinide/lanthanide (An/Ln) separations in nuclear waste streams. Finally, future research directions and prospects for these four separation methodologies are discussed.

2 Solvent extraction separation

Solvent extraction is one of the most competitive separation technologies, renowned for its high selectivity, cost-effectiveness, and operational convenience [26, 27] (Fig. 2a–b). It has been extensively applied to the separation of metal ions in complex matrices, with particular success in partitioning An and Ln from nuclear waste streams [28]. Established processes like PUREX [29] (Fig. 2c) and TALSPEAK [12] (Fig. 2d) exemplify the use of solvent extraction for An separation, solidifying its status as the most commercially viable and promising method for An/Ln separation from nuclear wastes [6, 30]. The extractant, a key component in the complex extraction process, plays a pivotal role. Given the high acidity of nuclear wastes, extractants designed for An separation must not only possess high efficiency and selectivity but also maintain excellent stability under highly acidic conditions [31].

The TALSPEAK process (Trivalent Actinide Lanthanide Separation by Phosphorus Reagent Extraction from Aqueous Complexes), developed in the 1970s, remains a benchmark for trivalent An(III)/Ln(III) separation [30, 32]. In its classical form, TALSPEAK employs the acidic organophosphorus extractant di-(2-ethylhexyl) phosphoric acid (HDEHP) in an organic diluent to extract lanthanides. Simultaneously, a water-soluble complexing agent (e.g., DTPA, lactate, or citrate) selectively retains trivalent actinides in the aqueous phase by forming stronger complexes [32]. Advanced variants like Advanced TALSPEAK [33], ALSEP (Actinide Lanthanide Separation Process) [17], and i-SANEX (innovative Selective ActiNide EXtraction) [34] improve selectivity and acid tolerance. These typically replace the lactate buffer with hydrophilic N-donor ligands (e.g., SO_3-Ph-BTP) or utilize combined extractants. Other significant separation processes include: DIAMEX (Diamide Extraction) for co-extracting An(III)/Ln(III); SANEX (Selective ActiNide Extraction) for subsequent An/Ln partitioning; GANEX (Group ActiNide EXtraction) for total actinide recovery[35]; and TRUEX for transuranic elements [36]. While a detailed comparison is beyond this review's scope, selected examples are discussed later.

Recent research has identified numerous highly selective extractants for An/Ln separation, including primary amines [37], pyridines [38], organophosphorus compounds [39], phosphor amides [40], calixarenes [41], and sulfur-containing extractants [42]. In solvent extraction, the amount of metal extracted is quantified by the distribution ratio

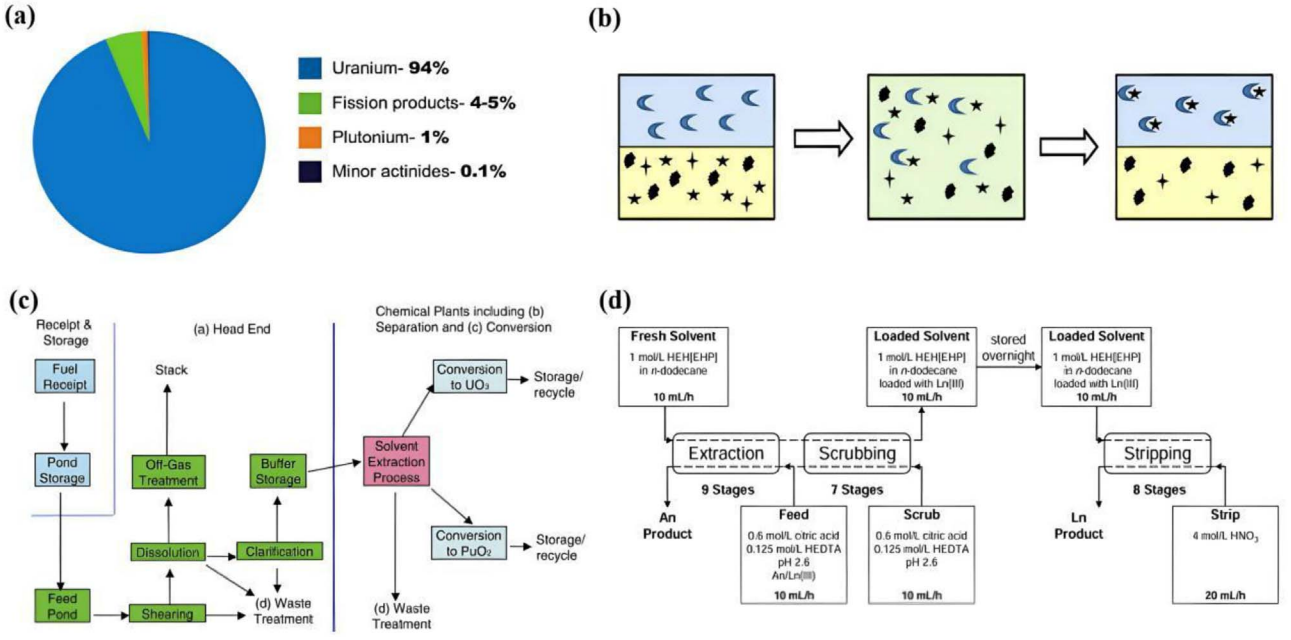


Fig. 2. (a) The general composition of SNF; (b) solvent extraction process [30]; (c) schematic representation of a typical configuration for an oxide fuel reprocessing plant using the PUREX process [43]; (d) flowsheet of the advanced TALSPEAK process demonstration test [44].

(D), defined as the concentration of the analyte in the organic phase to its concentration in the aqueous phase. For radioactive species, the radioactivity (A) of each phase is often used instead of concentration, as radioactivity is proportional to concentration and is typically easier to measure. To quantify the separation efficiency in liquid-liquid extraction, the SF is evaluated. The SF is the ratio of the distribution ratios of the elements to be separated. In this context, the distribution ratio of the actinide (D_{An}) is the numerator, while that of the lanthanide (D_{Ln}) is the denominator. Therefore, an SF $>$ 1 indicates preferential extraction of the D_{An} over the D_{Ln}, while an SF $\leq$ 1 indicates no separation [42].

Sulfur-containing extractants, centered on selective sulfur-actinide interactions, represent the most effective method currently known for separating trivalent An(III) from Ln(III) in a single step. These extractants preferentially transfer An(III) to the organic phase, leaving Ln (III) primarily in the aqueous phase [42]. Their primary mechanisms are solvation and cation exchange. Solvating extractants are neutral polar molecules that solvate metal ions in the organic phase when the metal is associated with appropriate anions to maintain neutral charge. Typically, solvating extractants exhibit high extraction efficiency at elevated acid concentrations and are stripped at lower acidities [42, 45, 46]. A representative example is carbamoylmethylphosphine sulfide (CMPS), extensively studied for its ability to non-selectively extract trivalent Ln and An from strongly acidic media in the Transuranium Extraction (TRUEX) process. Matloka et al. [47] synthesized various CMPS derivatives via the condensation of 2-(diphenylthiophosphoryl) acetic acid with different amine substituents (Fig. 3a–b). These demonstrated exceptional separation capability, achieving ~100% extraction of Th(III) while extracting less than 20% of La(III), Ce(III), Nd(III), Eu (III), and Yb(III) (Fig. 3d–e). However, CMPS exhibits limited An/Ln separation in 1 M HNO_3, likely due to splitting of the organic phase into two distinct phases. Aleksenko et al. [48] investigated the mechanism using Pd(II) and Re(I), finding that both metals formed M–S and M–O bonds with CMPS. This indirectly explained the performance decline in 1 M HNO_3 and suggested that adding synergistic agents could modify interfacial properties or influence aggregation and micelle formation, potentially mitigating the issue [46, 47].

Cation exchange extractants possess acidic functional groups that exchange protons for metal cations from the aqueous phase into the organic phase. Consequently, they exhibit high extraction efficiency under low acidity conditions and are stripped at higher acidities [45, 46, 49]. Prominent examples include bis(2-ethylhexyl) monothiophosphoric acid (HDEHTP) and bis(2-ethylhexyl) dithiophosphoric acid (HDEHDTP), which are among the most widely studied [42, 50]. Pattee et al. [51] were the first to use HDEHTP and HDEHDTP for An/Ln separation. They found that HDEHDTP offered a higher SF (SF = 2.55) in nitric acid compared to HDEHTP (SF = 0.89), while D values for both were consistent at ~0.06 within their respective optimal pH ranges (pH = 1.7–3.6 for HDEHDTP and pH = 0.8–1.9 for HDEHTP) [52]. Jensen et al. [53] synthesized Cyanex-301, which preferentially chelates Am(III) with an extraordinary $SF_{Am/Eu}$ exceeding 1000. However, a significant drawback for industrial application is its oxidative degradation under oxidizing conditions, gradually converting to Cyanex-302 and ultimately Cyanex-272, which substantially reduces selectivity [54]. This necessitates its use

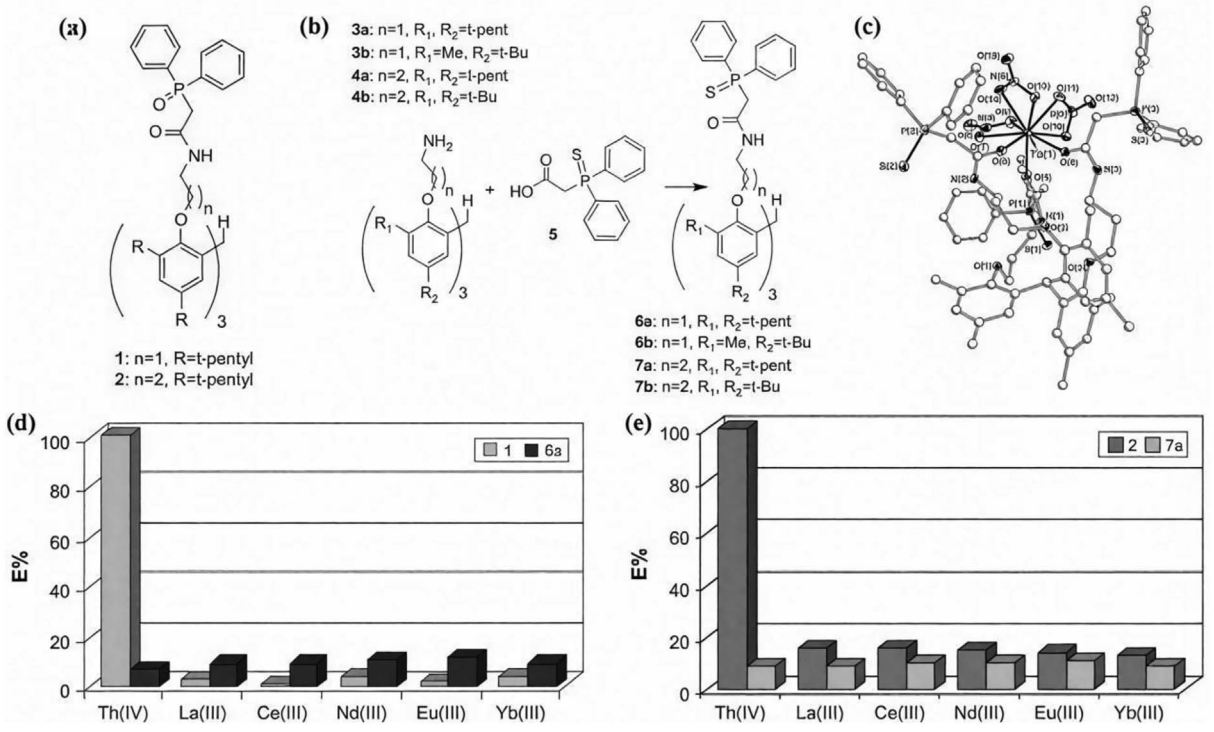


Fig. 3. (a) Tris-carbamoylmethylphosphine oxide (tris-CMPO); (b) synthetic protocol for the synthesis of tris-CMPS extractants; (c) diagram of one of the two symmetry independent terbium complexes in the structure of $[7a{\cdot}Tb(NO_3)_3]$; (d) comparison of metal binding by ligands 1 and 6a expressed by extraction percentage (%E); (e) comparison of metal binding by ligands 2 and 7a [47].

in combination with O-donor or N-donor ligands to suppress oxidation. For instance, Bessen et al. [22] and Wyrzykowski et al. [55] employed thioethers as sulfur extractants. The stronger C–S bond compared to P–S bonds maintains metal coordination to sulfur sites even in nitric acid, and thioethers generally require strong oxidants for degradation, making them less susceptible to oxidation by concentrated nitric acid.

Organophosphorus extractants, as a mature class of industrial reagents, are widely used for An/Ln separation in spent fuel reprocessing due to their strong extraction capability and low cost [1] (Fig. 4a). Traditional types include acidic and neutral organophosphorus extractants (Fig. 4b). Recently, researchers have incorporated these extractants onto pre-organized organic or inorganic scaffolds, creating rigid organophosphorus extractants with a superior extraction capacity and high selectivity for An [35]. These extractants typically feature highly charged P=O or P=S groups, which exhibit a strong coordination affinity for f-block elements, thereby enhancing the extraction efficiency [42]. The high reactivity and strong bonding capacity of phosphorus atoms impart strong polarity to the P=O/P=S bonds, making the steric and electronic effects more tunable and enabling the selective extraction of specific metal ions [56]. Furthermore, the alkyl or aryl side chains enhance the lipophilicity and solubility in organic solvents, increasing the saturation capacity [56]. Yang et al. [1] investigated the An separation capabilities of tributyl phosphate (TBP), α,α-di(2-ethylhexyl) phosphoric acid (HDEHP), octyl(phenyl)-*N*,*N*-diisobutylcarbamoylmethylphosphine oxide (CMPO) and trialkylphosphine oxide (TRPO). Their structural and mechanistic analyses elucidated the extraction mechanism at the molecular level and proposed design strategies for novel organophosphorus extractants [57]. Hill et al. [58] studied purified Cyanex-301, Cyanex-302, and Cyanex-272 for Am separation from ^{152}Eu. By investigating synergistic mixtures and slope analysis, they determined the optimal molar ratio to achieve $SF_{Am/Eu} \approx 10$. Additionally, Yang et al. [59] enhanced the nitric acid extraction performance of phosphine oxide ligands modified with O-donor atoms, improving their suitability for industrial flowsheets. Recognizing the performance decline of organophosphorus extractants in nitric acid, researchers have often modified them with O- or N-containing branches. For example, Horwitz et al. [36] and Goldberg et al. [60] reported O-modified carbamoylmethylphosphonates (CMPs) and carbamoylmethylphosphine oxides (CMPOs) used in the TRUEX process. These form six-membered chelate rings with metal cations, acting as internal buffers by coordinating protons, thereby improving their performance in nitric acid.

Despite their excellent separation capabilities, sulfur-based and organophosphorus extractants pose serious environmental concerns during reprocessing processes. Nitrogen-based extractants, however, generate cleaner residues. Nitrogen-containing extractants (composed solely of H, C, N, and O atoms) yield cleaner residues and are therefore prioritized in current nuclear processing engineering [17, 61, 62]. Most N-donor ligands in these extractants feature

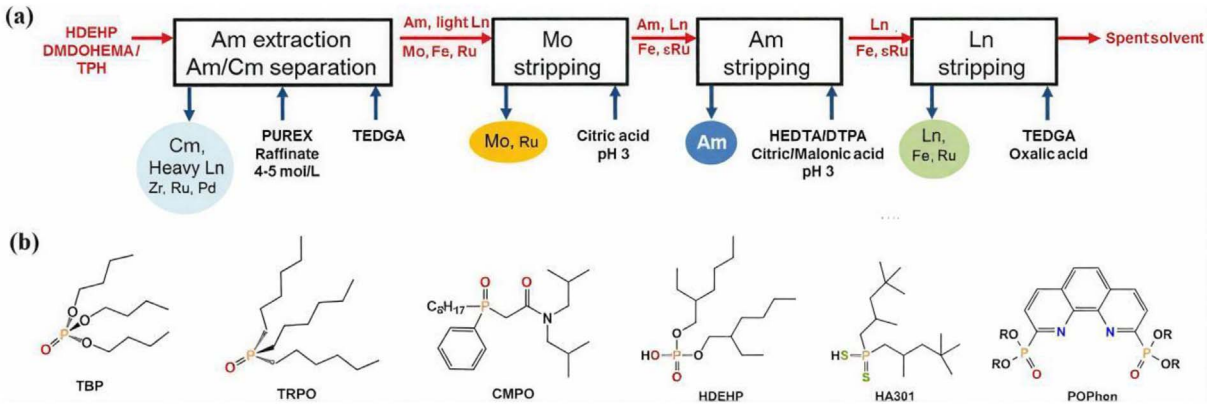


Fig. 4. (a) Flowsheet of actinide/lanthanide separation using organophosphorus extractants [35]; (b) representative Organophosphorus Extractants [1].

pyridine, pyrimidine, and benzimidazole moieties or are incorporated into aromatic rings. For example, Zhang et al. [63] synthesized *N*,*N*′-diethyl-*N*,*N*′-ditolyl-2,9-diamide-1,10-phenanthroline, and Wei et al. [64] synthesized pyridine dicarboxylic acid derivatives, both of which achieved SF > 10. Wang et al. [65] developed novel asymmetric phenanthroline ligands with pyrazole and amide groups, leveraging mixed N/O donor effects, and achieved $SF_{Am/Eu}$ = 34.5 in 1 M HNO_3 (Fig. 5a). Furthermore, Wang et al. [66] designed unsymmetrical phenanthroline diamide (DALPhen) via partial lactamization, balancing rigidity and solubility, and achieved $SF_{Am/Eu}$ = 100 in 2 M HNO_3 (Fig. 5b). These extractants commonly employ pyridine-diamide as mixed N,O-donor ligands, where the soft nitrogen atom of the pyridine group imparts An(III) selectivity over Ln(III), and the oxygen atom of the amide group ensures a strong metal affinity [67, 68]. Furthermore, organophosphorus and sulfur extractants suffer performance degradation under strong nitric acid and high-radiation fields [29]. To address this issue, researchers have anchored N-donor atoms to macrocyclic or rigid platforms. For instance, Cai et al. [6] synthesized five novel pillar [5] arene-based extractants by attaching multiple pyridinediamide groups, achieving $SF_{Am/Eu}$ > 11 in strong acid and retaining performance after exposure to 250 kGy of γ-radiation. Gao et al. [69] synthesized completely preorganized bis-lactam-1,10-phenanthroline (BLPhen) ligands featuring benzyl-stabilized frameworks and varying alkyl chain lengths. These highly stabilized ligands enhance acid stability and actinide affinity, demonstrating exceptional Am(III)/Eu(III) extraction and separation performance, with maximum SF ($SF_{Am/Eu}$) of 68 and 53. Cai et al. [28] further enhanced this by attaching the multidentate N-donor ligand 2,6-bis(1,2,4-triazol-3-yl) pyridine (PyTri) as hydrophobic pendants to the pillar [5] arene platform (Fig. 5c), creating an extractant with ten PyTri groups that achieved an exceptional $SF_{Am/Eu}$ of 172 in 1 M HNO_3 (Fig. 5d). Xiu et al. [18] incorporated phenyl rings into phenanthroline diamide ligands, leveraging the AAS effect (where aryl substitution enhances ligand-actinide binding [70, 71]), achieving $SF_{Am/Eu}$ = 53 in 4 M HNO_3. These modifications enable nitrogen-containing extractants to maintain outstanding performance under harsh acidic and radiative conditions, circumventing the problems associated with sulfur- and phosphorus-containing extractants.

Although conventional solvent extraction achieves satisfactory extraction and separation performance, it often faces issues such as environmental pollution and extractant deactivation problems. Consequently, researchers have integrated solvent extraction with other technologies to develop novel approaches. Mincher et al. [72] proposed introducing supercritical fluid technology (Fig. 6a–b). Since carbon dioxide is an excellent solvent for fluorinated and phosphate ligands, including traditional TBP used for industrial-scale uranium separation, supercritical carbon dioxide ($scCO_2$) can replace conventional acidic aqueous phases and organic solvents, eliminate subsequent liquid waste disposal and reduce environmental risks (Fig. 6c). For example, Koegler et al. [73] used $TBP(HNO_3)_{1.8}(H_2O)_{0.6}$ in $scCO_2$ to extract uranium and gadolinium from light-water reactor fuel, achieving up to 98% uranium extraction with less than 1% plutonium co-extraction from actinide mixtures under 3 M HNO_3 conditions. The separation of neptunium and americium was also demonstrated under similar conditions [74]. Geist et al. [34] reported a novel i-SANEX (innovative Selective ActiNide EXtraction) process based on hydrophilic ligands. This process operates without buffers or salting-out agents in the aqueous phase and maintains good separation efficiency even in 2 mol/L HNO_3. For instance, Wu et al. [2] employed the *N*,*N*,*N*′,*N*′-tetraoctyl diglycolamide (TODGA) ligand within the i-SANEX framework to separate actinides, achieving an impressive $SF_{Eu/Am}$ of 395.97 in 2 M HNO_3. Furthermore, Zhou et al. [75] employed acidic phosphoric chitosan (aPCS) as a complexing agent in shear-induced dissociation-ultrafiltration (SID-UF) for sequential Pr(III)/Nd(III) separation. By exploiting differences in coordination strength, they achieved a SF of 12. The SID-UF technique employs shear stress to mitigate membrane fouling, enables efficient metal-ion separation, and permits complexing agent recovery without acid decomplexation – simplifying the process and reducing operational costs (Fig. 6d).

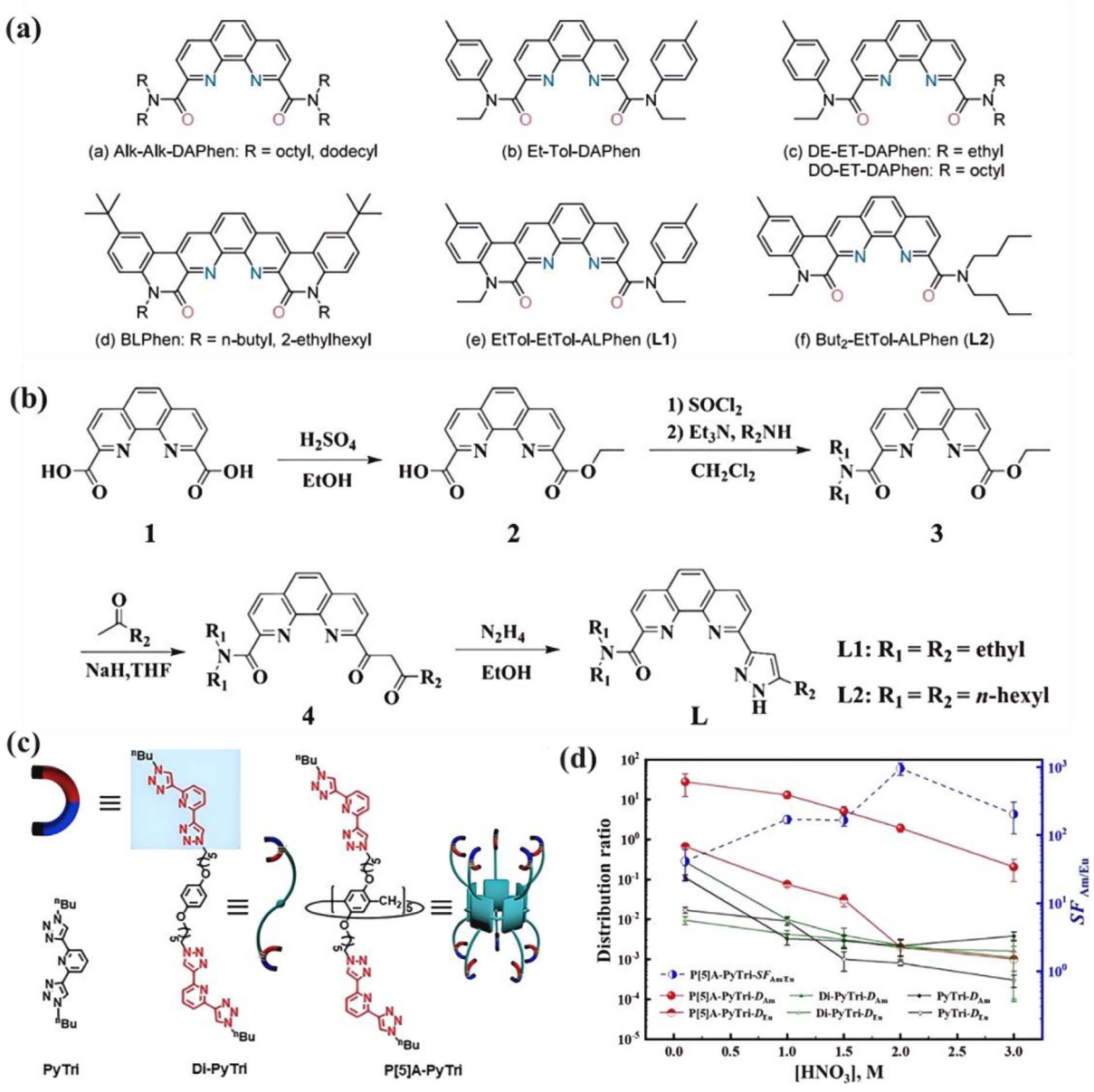


Fig. 5. (a) Molecular structures of phenanthroline-derived extractants [66]; (b) asymmetric tetradentate phenanthroline chelators with pyrazole and amide groups [65]; (c) chemical structures and cartoon representations of PyTri, Di-PyTri, and P[5]A-PyTri; (d) effect of HNO_3 concentration on extraction of Am(III) and Eu(III) [28].

Solvent extraction technology, leveraging its high selectivity, operational convenience, and mature industrial applications (e.g., PUREX and TALSPEAK), remains the most competitive method for An/Ln separation from nuclear wastes. However, extraction agents currently face bottlenecks such as acidity sensitivity, oxidative degradation, and poor radiation stability. Therefore, next-generation extraction technologies should synergistically optimize three key objectives through molecular design: 1) Enhance stability under extreme conditions (strong acid/high radiation) through rigid, multidentate ligands; 2) Break through selectivity limits by exploiting An-specific coordination mechanisms (e.g., soft N-donors, AAS effect); 3) Develop fully green systems (e.g., biodegradable ligands/solvent-free extraction) to eliminate environmental risks associated with nuclear waste processing. Concurrently, innovative processes (e.g., coupling supercritical fluids with intelligent separation schemes) offer significant promise for advancing separation technology towards enhanced efficiency and sustainability.

3 Crystallization separation

Despite significant progress in multi-step solvent extraction processes like PUREX for uranium extraction and single-step processes like GANEX, several persistent challenges remain. These include difficulties in separating MAs such

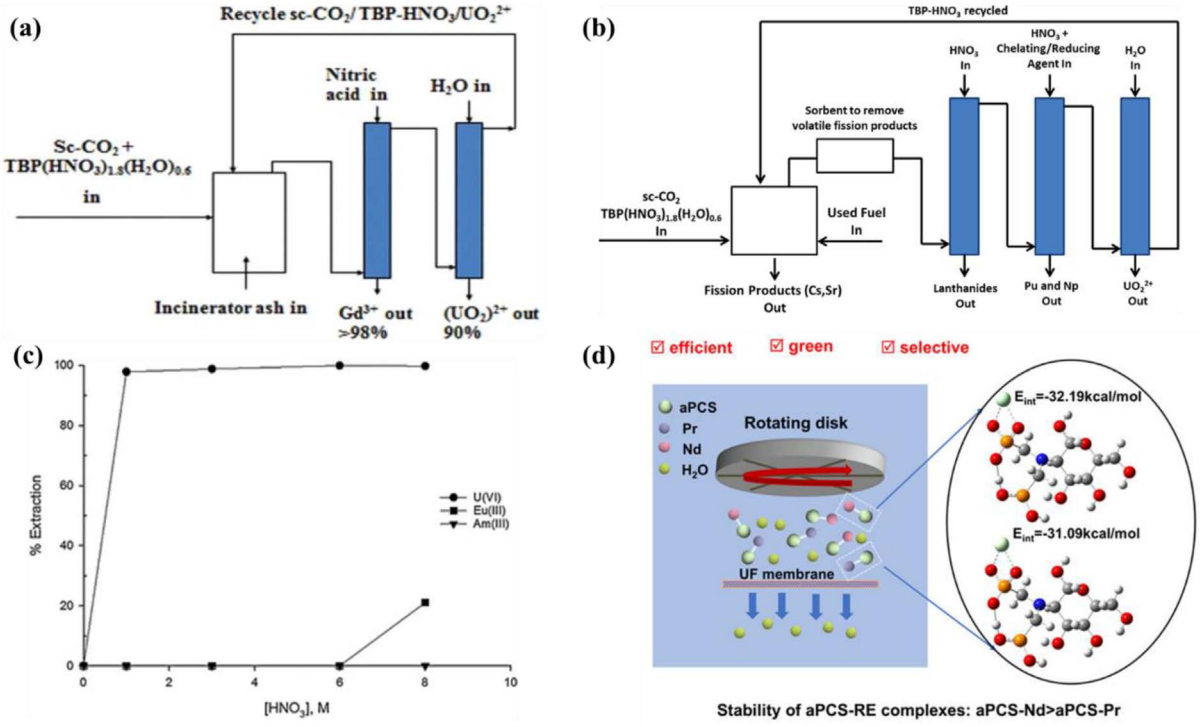


Fig. 6. (a) $scCO_2$ dissolution of uranium and gadolinium oxides from incinerator ash, followed by selective stripping and countercurrent elution; (b) conceptual flowsheet for recovering uranium from spent fuel using $scCO_2$ extraction; (c) $scCO_2$ extraction of UO_2^{2+}, Eu^{3+} and Am^{3+} ions from nitric acid solutions with TBP [72]; (d) schematic diagram of selective separation of ternary mixed rare earth ions by shear induced dissociation coupling with ultrafiltration (SID-UF) [75].

as Np and Am [76, 77], the inherent complexity and stringent control requirements of extraction processes (which involve extraction, scrubbing, and stripping), and the generation of substantial secondary nuclear waste associated with the use of organic solvents [10, 76, 78]. Consequently, alternative separation methods are urgently needed to address these challenges. Crystallization offers a promising alternative by leveraging differences in solubility and crystallization behavior for selective separation. This approach simplifies the process, reduces organic waste, and can directly yield high-purity solids, thereby avoiding challenges associated with solvent extraction. The most extensively researched strategy is "oxidation followed by separation." This commonly involves initial oxidation within a solution using strongly oxidizing acids (e.g., nitric acid and bismuthic acid), followed by separation via crystallization techniques [10, 79, 80]. Due to their higher atomic number, An exhibit expanded valence electron orbitals resulting from reduced shielding of the outermost 5f electrons, enabling access to multiple oxidation states. Spherical actinide ions [e.g., U(VI), Pu(VI), Np(VI), Am(VI)] can be oxidized to form linear dioxo actinyl cations (e.g., UO_2^{2+}, PuO_2^{2+}, NpO_2^{2+}, AmO_2^{2+}), while Ln, with the exception of Ce, remain trivalent [10, 79, 81]. This oxidation state differentiation provides a novel basis for separating An from Ln. Researchers have thus developed crystallization separation techniques that exploit the resulting differences in coordination behavior, solubility, or crystallization tendencies between the oxidized An and trivalent Ln [80, 82, 83] .

This separation approach employs specifically designed organic or inorganic ligands with complex and tunable properties to enhance the differences in lattice formation and coordination chemistry between Ln and An elements. This amplification leads to divergent crystallization behaviors, enabling the production of high-purity crystalline products through simple solid-liquid filtration [9]. The application of this technology in fuel reprocessing began in the 1980s. Kikuchi et al. [84] first described selective crystallization for SNF reprocessing, demonstrating the effective separation of plutonium from uranium and other fission products via plutonium co-crystallization. Wang et al. [85] demonstrated the selective crystallization of Eu^{3+} as an oxalate complex in the presence of UO_2^{2+}, showcasing its potential for separating Ln(III) from An(VI). While these studies validated the feasibility of crystallization separation, the relatively low separation efficiency was insufficient to meet the demands for high-performance partitioning. To address this, Gao et al. [11] exploited the solubility differences of actinide and lanthanide oxides in inorganic salt solutions. They achieved near-complete dissolution (~100%) of lanthanide oxides using an $AlCl_3$ solution at 75 °C, while coexisting actinide oxides remained largely insoluble, achieving SF as high as $SF_{Ln/U} = 1630$. Crucially, the $AlCl_3$ solution maintained 95.5% of its dissolution capacity after three dissolution/precipitation cycles, indicating strong potential for industrial application. Li et al. [86] introduced the ligands 3,6-di-2-pyridyl-1,2,4,5-tetrazine (L1) and its hydrolysis product pyridine-2-carbaldehyde

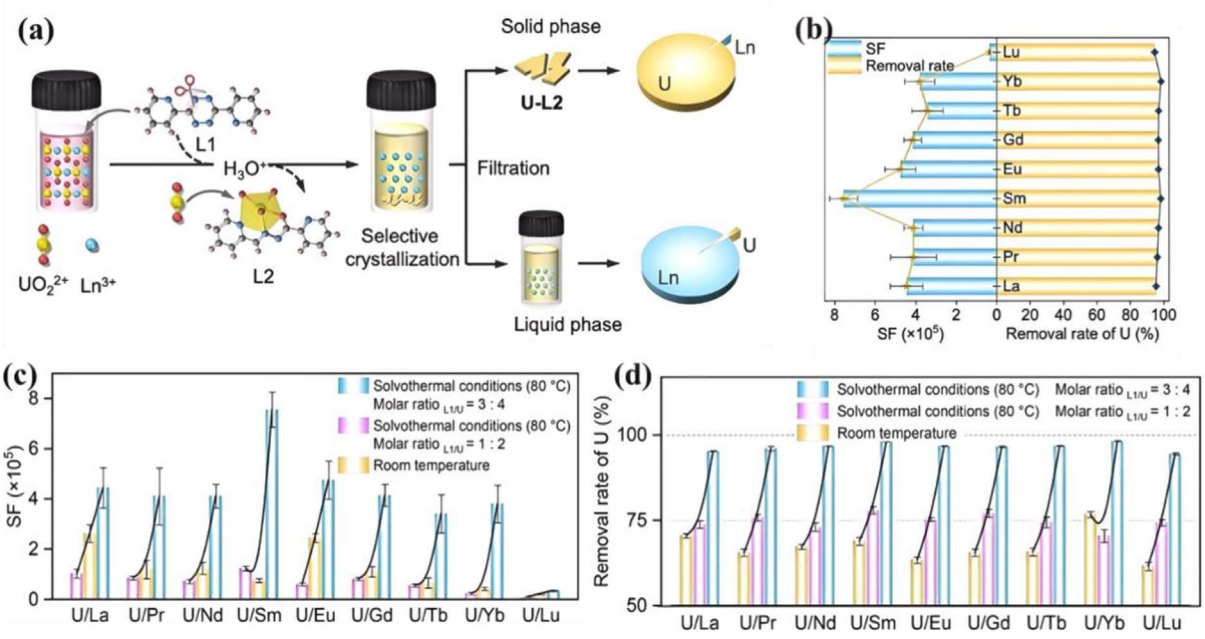


Fig. 7. (a) A schematic representation showing the separation strategy of U and Ln through fractional crystallization; (b) the SF of U/Ln and removal rates of U; (c) SF for the binary U/Ln (Ln = La to Lu) systems; (d) removal rates of U in the binary U/Ln (Ln = La to Lu) system [86].

(pyridine-2-carbonyl) hydrazone (L2) (Fig. 7a). Employing fractional crystallization techniques, they achieved crystallization efficiencies exceeding 98% and an extraordinary $SF_{U(VI)/Sm(III)}$ of 756,276 which is the highest value reported. Remarkably, crystallization efficiencies remained above 62% and $SF_{U/Ln}$ exceeded 23,037 even under varying ambient temperatures (Figs. 7b–7d). Considering the impact of the highly acidic environment in spent fuel reprocessing on crystallization. It is important to note that this high selectivity relies on the distinct linear geometry of UO_2^{2+} compared to spherical Ln^{3+} ions, which is a different separation mechanism from the covalent differentiation used for An(III)/Ln(III) separation. Nevertheless, it demonstrates the potential of crystallization for recovering high-valent actinides. Wang et al. [9] synthesized an N/O-donor ligand, (E)-N′-(pyridin-2-ylmethyl) pyridinehydroxymidoyl (PYPH). This ligand features a planar coordination mode and enables the selective crystallization of U(VI) from acidic solutions containing complex mixtures of lanthanide ions. Due to its exceptional acid resistance, SF exceeding 100 were achieved for binary Ln(III/IV)/U(VI) systems at pH = 3 and in 0.1 M HNO_3, facilitating effective An/Ln separation in SNF waste.

In summary, while crystallization separation shows promise for partitioning actinides (An), particularly in higher oxidation states like U(VI), from lanthanides (Ln), research in this field remains at a relatively early stage. However, it offers a novel approach distinct from solvent extraction for partitioning and transmutation (P&T) of high-level liquid nuclear waste (HLLW) and may help address some limitations encountered in solvent extraction. Systematic reports specifically focusing on Ln/An separation via crystallization, especially for trivalent minor actinides versus lanthanides, are still limited. This highlights the necessity for deeper exploration. A notable challenge lies in the design of specific ligands capable of efficiently and selectively separating key actinides, such as UO_2^{2+}, from all lanthanide ions [87–89]. Furthermore, the stringent requirements imposed by the spent fuel reprocessing environment, including extremely high selectivity, product purity, and strong acid resistance, remain primary bottlenecks hindering the practical engineering application of crystallization separation technology [90]. However, through sustained efforts to address these key scientific and technical challenges, crystallization separation holds significant potential to become a core method for the efficient separation of An from Ln in next-generation advanced nuclear fuel cycles.

4 Adsorption separation

While crystallization separation addresses the issue of secondary pollution inherent in traditional liquid-liquid extraction, it imposes stringent structural requirements on ligands. The harsh environment of spent fuel reprocessing further complicates the synthesis of ligands suitable for crystallization, hindering its development. Compared to crystallization, adsorption separation offers distinct advantages with its simpler operation, flexible ligand design, and ease of combination with robust solid supports, presenting unique application potential. Adsorption separation imposes lower structural demands on ligands and features simpler and more versatile preparation procedures. Consequently, researchers have focused on this method. Adsorption separation relies on solid-phase adsorbents functionalized with specific groups (e.g., amide groups) or

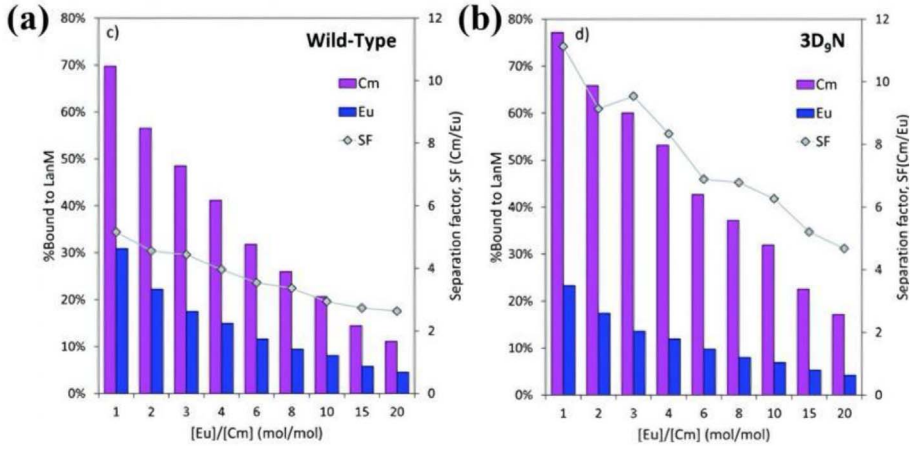


Fig. 8. Binding capacity and SF for Cm and Eu by (a) wild-type and (b) $3D_9N$ variant [7].

polymers (e.g., functionalized resins) designed for the selective adsorption of An [91]. This approach allows the use of carriers composed of materials resistant to strong acids and radiation, enabling stable operation under the demanding conditions of spent fuel reprocessing. Joseph et al. [7] demonstrated the feasibility of this approach using the naturally occurring protein lanmodulin (LanM), which exhibits exceptional selectivity for An over Ln, achieving SF exceeding 10 (Fig. 8a–b). Gujar et al. [92] fabricated polyethersulfone (PS)-based composite polymer beads containing TODGA via phase inversion technology. The incorporated TODGA modulated the adsorption behavior towards An like UO_2^{2+} and Np^{4+} without significantly affecting Am^{3+} adsorption, enabling the selective separation of Am^{3+} from Ln with high SF ($SF_{U/Am} = 880$, $SF_{Np/Am} = 8.77$).

In addition to the novel materials discussed above, well-established extraction chromatography resins (e.g., TEVA, TRU, DGA, and LN resins from Eichrom/Triskem) are widely used for analytical and small-scale separations of actinides and lanthanides [91, 92]. These resins consist of an inert support (e.g., silica or acrylic polymer) impregnated with a selective extractant (e.g., CMPO, DGA, HDEHP). They offer excellent batch-to-batch reproducibility, good radiation stability (up to several hundred kGy), and ease of operation in column mode. For example, DGA resins have been shown to effectively separate Am (III) from Ln(III) in nitric acid media with SF in the range of 10–100 depending on acidity [92]. However, their relatively slow kinetics and limited throughput in high-concentration feeds remain challenging for large-scale implementation [91].

Although the aforementioned adsorbents achieve effective An/Ln separation, their reliance on conventional polymers or biological materials, such as proteins, limits their applicability in high-radiation fields. Fortunately, the adsorbents used in adsorption separation can be modified or combined with other materials to overcome the challenges posed by strong acids and intense radiation [20, 93]. Carbon-based materials such as graphdiyne, graphene, and carbon nanotubes (CNTs) represent promising candidates. For instance, Yuan et al. [94] successfully demonstrated the potential of graphdiyne for adsorption separation by selectively adsorbing Th^{4+}. Huang et al. [8] characterized a three-dimensional graphene structure spectroscopically, revealing that its abundant oxygen- and nitrogen-containing functional groups confer excellent adsorption capacity for Eu(III) (~150 mg/g) and Th(IV) (~220 mg/g). They further enhanced the utility of graphene by loading it onto polyethyleneimine composite aerogel (GO-PEI), creating a material capable of selectively adsorbing and enriching uranium ions from solutions with a remarkable rejection rate of 99% [95]. Shao et al. [96] achieved an astonishing adsorption capacity of 1960 mg/g for uranium by modifying graphene oxide with polyaniline. Sharma et al. [13] developed a highly radiation-resistant adsorbent, PS-DGA-MWCNT, by incorporating diglycolamide-functionalized multi-walled carbon nanotubes (DGA-MWCNTs) into a polyether sulfone (PS) matrix (Fig. 9a–b). This composite material maintained excellent separation performance even after exposure to 500 kGy of γ-radiation, demonstrating its capability for effective An/Ln separation in SNF waste streams (Fig. 9c–d).

However, while adsorption separation effectively mitigates the influence of high-radiation environments and avoids the pollution issues associated with liquid-liquid extraction, it faces challenges related to adsorption kinetics and relatively low throughput. This can result in slow separation efficiency and slow kinetics, which is particularly problematic when processing feeds containing high concentrations of metal ions. Subsequent efforts should therefore focus on developing novel adsorbent materials with enhanced adsorption rates and higher processing capacities (e.g., by optimizing pore structures and improving mass transfer efficiency) or on designing more efficient separation processes (e.g., continuous-flow fixed beds, membrane separation modules). Additionally, in-depth investigation into the mechanisms of selective and competitive adsorption behaviors within complex, high-concentration systems is crucial to overcome kinetic limitations and enhance separation efficiency and throughput in practical applications.

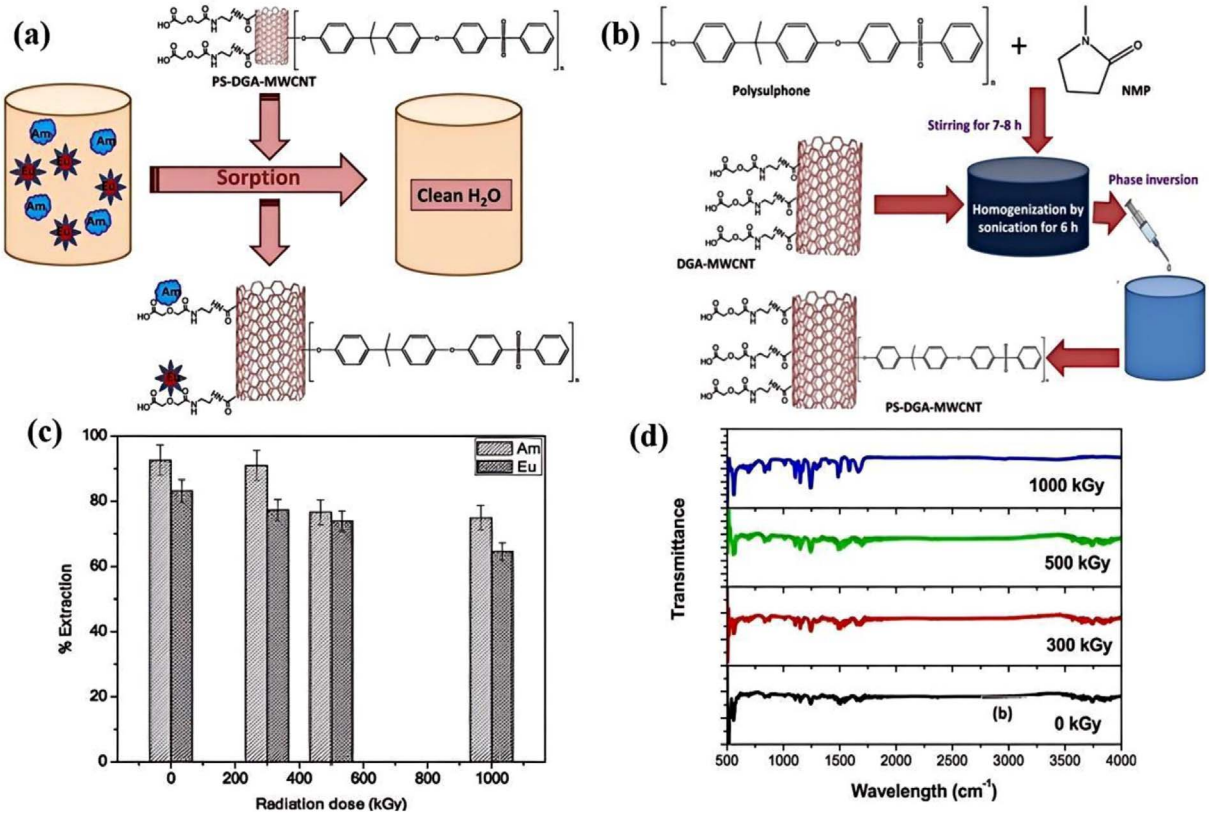


Fig. 9. (a) Schematic of selective adsorption process by PS-DGA-MWCNT functionalized composite; (b) schematic representation of the synthesis of the DGA-CNT-functionalized polysulfone polymeric beads; (c) effect of radiation exposure on the extraction of Am^{3+} and Eu^{3+} by the PS-CNT; (d) FTIR spectra for irradiated and unirradiated PS- DGA-MWCNT [13].

5 Membrane separation

While adsorption separation has successfully mitigated the challenges of strong acidity and high radiation in An/Ln separation through the substitution or incorporation of functional materials into the adsorbents, membrane separation offers distinct advantages. Compared to adsorption, membrane separation exhibits lower mass transfer resistance, reduced energy consumption, and potential for continuous operation, resulting in higher separation efficiency.

Membrane separation applied to An/Ln partitioning in spent fuel reprocessing primarily relies on two separation mechanisms: 1) Size-Sieving Mechanism: This approach exploits differences in the hydraulic diameter of actinide and lanthanide species for selective rejection through membrane pores. This strategy's success critically depends on the pretreatment of the stream to oxidize An into linear actinyl ions (e.g., AnO_2^{2+}). The resulting hydrated actinyl ions are substantially larger than their spherical Ln^{3+} counterparts, a difference that is further amplified and serves as the key physical basis for efficient membrane-based sieving. Porous carbon materials and organic framework materials with narrow, well-defined pore size distributions hold significant promise [97]. Chen et al. [98] synthesized Graphene Oxide Membranes (GOMs) with unique nanolayered structures, offering advantages such as strong mechanical stability, controllable dimensions, and ease of fabrication [99, 100]. The interlayer spacing (and thus effective pore size) of GOMs can be precisely tuned via physical confinement or cation intercalation. Crucially, treatment with strong oxidizing agents converts An into linear dioxo actinyl cations (e.g., AnO_2^{n+}), while Ln retain their spherical trivalent ionic state, creating a significant difference in spatial dimensions (Fig. 10a–b). Leveraging this, Wang et al. [79] developed a GOM capable of sieving An from Ln under highly acidic conditions, achieving an impressive SF ($SF_{Ce/U}$) of 400 (Fig. 10c). Furthermore, the GOM's separation performance remained largely unaffected after exposure to 100 kGy of γ-radiation in 3.0 M HNO_3 solution. Additionally, Zhang et al. [87] developed nanoscale polyoxometalate (POM) clusters with structural vacancies. These clusters selectively coordinate with hexavalent An in nitric acid to form larger actinide-POM clusters, amplifying the size difference between An and Ln ions. By immobilizing these POMs onto commercially available ultrafiltration membranes, they achieved An/Ln separation via ultrafiltration [101–103], with rejection rates exceeding 90% for ions such as U, Pu, and Am. Liu et al. developed a series of metal-organic framework (MOF) membranes with tunable pore apertures by systematically modulating ligand architectures, metal species, defect engineering, and crystal orientation (e.g., MOF-808 (10.1Å) [104] (Fig. 11a), UiO-66 (10.1 Å) [105] (Fig. 11b), MIP-177-LT (11Å) [106] (Fig. 11c) and MIP-201 (10.5 Å) [107] (Fig. 11d)). These

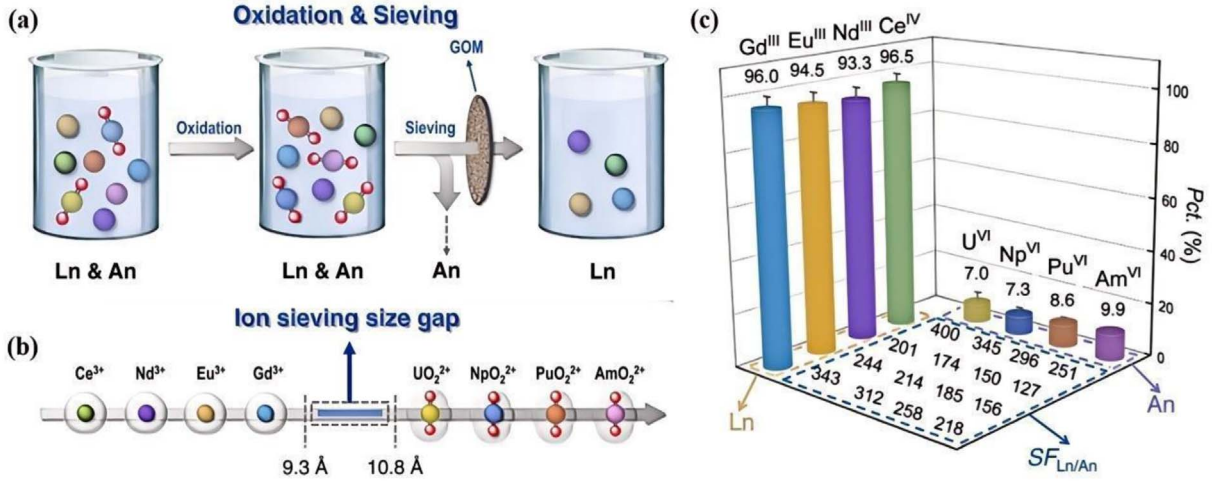


Fig. 10. (a) Schematic diagram showing actinide–lanthanide group separation via the ion-sieving strategy; (b) size comparison of representative lanthanide and actinide ions; (c) separation results of a mixed An/Ln waste solution after sieving through the GOM [79].

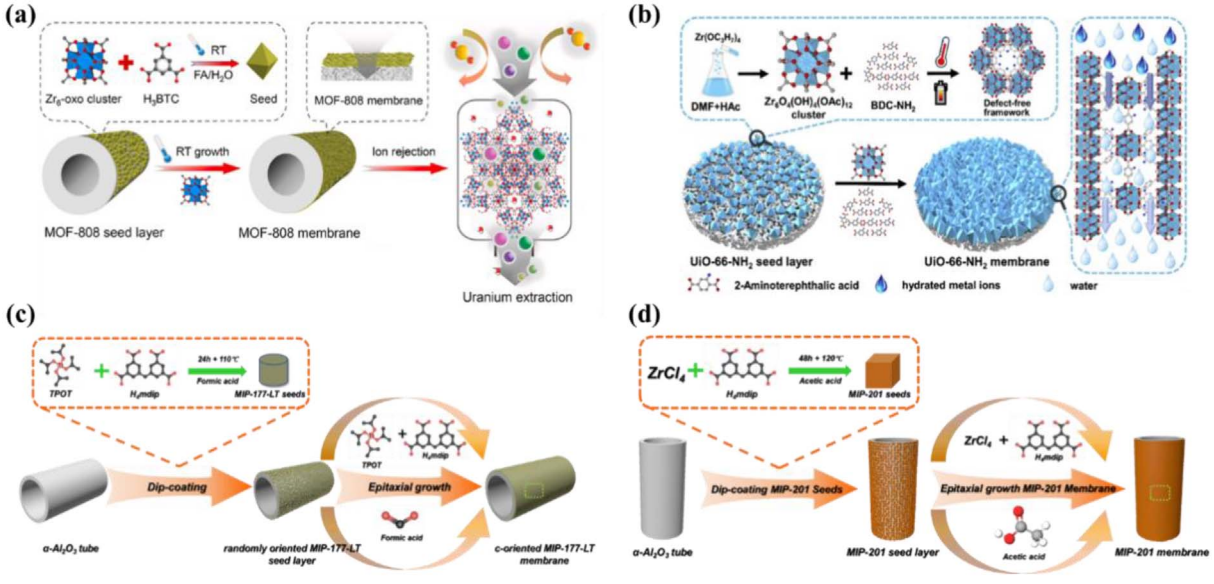


Fig. 11. (a) Schematic illustration of RT synthesis of MOF-808 membrane [104]; (b) schematic representation of defect-free UiO-66-NH_2 membrane fabrication [105]; (c) schematic illustration of the synthesis of the MIP-177-LT membrane [106]; (d) schematic illustration of the synthesis of the MIP-201 membrane [107].

membranes demonstrated exceptional ion-sieving capabilities, confirming that structural control enabled precise size-based separation through uniform nanochannels. It should be noted that the size-sieving strategy is inherently dependent on the controlled oxidation state of actinides (An). However, stabilizing Am(III)/Cm(III) in their oxidized forms typically requires strongly acidic conditions. Consequently, membranes employed in size-sieving-based separation must exhibit robust acid resistance and oxidation stability to be viable for An(III)/Ln(III) separation. 2) Complexation/Coordination Mechanism: This strategy involves developing functionalized membrane materials modified with specific chemical groups (e.g., phosphoric acid, phosphonate, and amidoxime) designed to selectively complex and retain An via chemical adsorption [108]. For example, Priyanka Suresh et al. [3] synthesized a poly (EGMP-co-HEMA) functionalized membrane, achieving a SF ($SF_{La/U}$) of 74 between La^{3+} and UO_2^{2+} at pH = 1.

In summary, membrane separation compensates for the limitations of adsorption separation, namely low throughput and insufficient capability for high-concentration feed solutions, through its core advantages of low mass transfer

Table 1. Comparison of representative An/Ln separation technologies under relevant conditions.

Method	Target ions	Feed acidity	Key material	SF (An/Ln)	Kinetics	Radiation stability	Reusability	Secondary waste	Scalability	Ref.
Solvent extraction (N-donor)	Am(III)/Eu (III)	1–4 M HNO_3	Phenanthroline diamide	~172	Fast (minutes)	>250 kGy	-	Organic solvent waste	High (industrial)	[6, 28]
Crystallization (U(VI)/Ln)	U(VI)/Sm (III)	0.1 M HNO_3	PYPH ligand	>100	Moderate (hours)	Not reported	-	Minimal (solid only)	Low (lab scale)	[9]
Adsorption	Am(III)/Eu (III)	0.01–3 M HNO_3	DGA-MWCNT@PS	~5	Slow (hours)	500 kGy	Yes	Minimal	Moderate	[13]
Membrane (size-sieving)	U(VI)/Ce (III)	3 M HNO_3	GO membrane	400	Fast (continuous)	100 kGy	Yes	Minimal	Moderate (module)	[78]
Membrane (complexation)	U(VI)/La (III)	pH=1	Poly(EGMP-co-HEMA)	74	Fast	Not reported	Not reported	Minimal	Low	[3]

resistance, low energy consumption, efficient separation mechanisms, and potential for continuous operation. However, both underlying separation mechanisms face inherent drawbacks: 1) Size-sieving requires complex feed pre-treatment to induce the necessary spatial size difference between An and Ln species. 2) Complexation-based functionalized membranes necessitate the development of organic ligands with a pronounced affinity for An, and the membrane modification process itself often suffers from uncertainties. Therefore, the future development of membrane materials should prioritize the following: 1) Industrialization Potential: Focusing on membrane performance metrics such as flux/permeability and separation efficiency. 2) Operational Stability: Ensuring membrane robustness under harsh conditions (e.g., resistance to strong acids/bases and high radiation fields). 3) Process Optimization: Streamlining often complex membrane fabrication procedures. Furthermore, given that spent fuel reprocessing constitutes a high-hazard operation, the introduction of new membrane separation technologies must be accompanied by improvements and rigorous monitoring of associated processing facilities and waste streams (gaseous, liquid, and solid) [23, 24].

6 Conclusion and outlook

The separation of An from Ln in nuclear waste streams is a core challenge in advancing sustainable nuclear energy. Solvent extraction, which leverages mature industrial applications (e.g., the PUREX process) and high selectivity (e.g., $SF_{Am/Eu} > 170$ for nitrogen-donor ligands in 1M HNO_3), remains the most competitive technology. However, it urgently requires breakthroughs to overcome the issues of organic waste pollution and extractant oxidative degradation. Crystallization separation achieves ultra-high SF ($SF_{U/Sm} > 7.5 \times 10^5$) and avoids solvent pollution through inorganic salt cycling (e.g., $AlCl_3$) or specific ligands (e.g., PYPH). Yet, its development is constrained by the limited acid resistance of the ligands and narrow applicability, particularly for the separation of An(III). Adsorption separation demonstrates excellent radiation resistance (stable up to 500 kGy) and environmental friendliness using functionalized materials (e.g., DGA-MWCNTs). However, slow adsorption kinetics significantly limit their efficiency in processing high-concentration systems. Membrane separation offers advantages such as low mass transfer resistance and the potential for continuous operation. GOMs maintain high selectivity ($SF_{Ce/U} = 400$ in 3M HNO_3) even under strong acid and radiation conditions. Nevertheless, its industrialization relies on complex pre-oxidation steps for An and uncertain membrane-modification processes.

Future research must focus on synergistic innovation across three key objectives: 1) Molecular Design: Develop functional materials integrating rigid, multidentate structures (e.g., ligands exploiting AAS effects) and soft nitrogen donors to enhance An(III)/Ln(III) selectivity and stability under extreme conditions (>4M HNO_3, >500 kGy). Intelligent design strategies should be implemented, utilizing molecular simulation and machine learning to predict ligand performance based on electronic structure and steric

hindrance, thus building targeted ligand families for actinide ions. 2) Process Innovation: Couple green technologies (e.g., supercritical CO_2 extraction, biomimetic adsorbents) to eliminate secondary waste, and implement multi-stage integrated strategies (e.g., membrane-crystallization hybrids) to overcome limitations of single technologies An intelligent "membrane sieving-adsorption/crystallization refining" process can be designed. It combines pre-oxidation and membrane sieving for coarse An(VI)/Ln(III) separation, followed by selective crystallization or adsorption for deep Am(III) purification, all managed by an integrated online monitoring and feedback control system for real-time optimization. 3) Engineering Optimization: Enhance mass transfer kinetics (e.g., hierarchically porous adsorbents), streamline membrane fabrication, and develop intelligent control systems. The transition to efficient, low-carbon, and practical separation technologies requires overcoming scale-up challenges with modular designs and validating candidate processes through life cycle assessments of their energy use, carbon footprint, and secondary waste to support the closing of the nuclear fuel cycle.

Acknowledgments

The authors are grateful to National Natural Science Foundation of China (22478056), JSPS KAKENHI (JP12345678) and Xing Yuan program of China National Nuclear Corporation (8208 of CNPE) for the financial support.

Conflicts of interest

The authors declare that they have no known competing financial interests or personal relationships that could have appeared to influence the work reported in this paper.

Data availability statement

Data will be made available on request.

Author contribution statement

Yue Zhang: Writing – original draft & review. Xiangcheng Jin: Writing – original draft & review. Meng Wang: Investigation, Writing –Draw charts. Kai Sun: Investigation, Writing – Draw charts. Meng Ge: Writing – review & editing, Supervision. Shinichiro Noro: Writing – review, Supervision. Yi Liu: Writing – review & editing, Supervision, Resources, Funding acquisition, Conceptualization.

References

1 X. Yang, L. Xu, A. Zhang, et al., Organophosphorus extractants: A critical choice for actinides/lanthanides separation in nuclear fuel cycle. *Chem. Eur. J.* **29**(33), e202300456 (2023).
2 Q. Wu, H. Hao, Y. Liu, et al., Selective separation of americium(III), curium(III), and lanthanide(III) by aqueous and organic competitive extraction. *Inorg. Chem.* **63**(1), 462–473 (2024).
3 P. Suresh, L. Johnson, C.E. Duval, Membrane adsorbers with copolymer coatings for the separation of actinides from lanthanides (UO_2^{2+} and La^{3+}). *Ind. Eng. Chem. Res.* **63** (46), 20373–20382 (2024).
4 K. Niu, F. Yang, T. Gaudin, et al., Theoretical study of effects of solvents, ligands, and anions on separation of trivalent lanthanides and actinides. *Inorg. Chem.* **60**(13), 9552–9562 (2021).
5 H.H. Dam, D.N. Reinhoudt, W. Verboom, Multicoordinate ligands for actinide/lanthanide separations. *Chem. Soc. Rev.* **36**(2), 367–377 (2007).
6 Y. Cai, S.A. Ansari, K. Fu, et al., Highly efficient actinide (III)/lanthanide(III) separation by novel pillar[5]arene-based picolinamide ligands: A study on synthesis, solvent extraction and complexation. *J. Hazard. Mater.* **405**, 124214 (2021).
7 J.A. Mattocks, J.A. Cotruvo, G.J.P. Deblonde, Engineering lanmodulin's selectivity for actinides over lanthanides by controlling solvent coordination and second-sphere interactions. *Chem. Sci.* **13**(20), 6054–6066 (2022).
8 Z. Huang, Z. Li, L. Zheng, et al., Adsorption of Eu(III) and Th(IV) on three-dimensional graphene-based macrostructure studied by spectroscopic investigation. *Environ. Pollut.* **248**, 82–89 (2019).
9 J. Wang, Y. Li, R. Yao, et al., Selective crystallization separation of uranium (VI) complexes from lanthanides. *Inorg. Chem.* **64**(1), 202–212 (2025).
10 Z. Wang, J. Lu, X. Dong, et al., Ultra-efficient americium/lanthanide separation through oxidation state control. *J. Am. Chem. Soc.* **144**(14), 6383–6389 (2022).
11 X. Gao, A. Ding, Y. Li, et al., Selective dissolution and separation of lanthanides and actinides from spent nuclear fuel using inorganic salt solutions: A sustainable approach. *Separation Purif. Technol.* **360**, 131035 (2025).
12 Y. Wang, G.J.P. Deblonde, R.J. Abergel, Hydroxypyridinone derivatives: A low-ph alternative to polyaminocarboxylates for TALSPEAK-like separation of trivalent actinides from lanthanides. *ACS Omega* **5**(22), 12996–13005 (2020).
13 D.B. Sharma, A. Sengupta, A.K. Singha Deb, et al., Diglycolamic acid-functionalized MWCNT-augmented polymeric beads for efficient separation of trivalent lanthanides and actinides. *Ind. Eng. Chem. Res.* **63**(31), 13814–13825 (2024).
14 H.Y. Tan, C.H. Yeong, Y.H. Wong, et al., Neutron-activated theranostic radionuclides for nuclear medicine. *Nucl. Med. Biol.* **90–91**, 55–68 (2020).
15 L. Liu, H. Guo, L. Dai, et al., The role of nuclear energy in the carbon neutrality goal. *Prog. Nucl. Energy.* **162**, 104772 (2023).
16 H. Hao, Q. Zheng, Y. Zhang, et al., Highly efficient group separation of hexavalent actinides from lanthanides through a biphasic cooperative extraction system. *J. Mol. Liq.* **389**, 122909 (2023).
17 A.V. Gelis, G.J. Lumetta, Actinide lanthanide separation process – ALSEP. *Ind. Eng. Chem. Res.* **53**(4), 1624–1631 (2014).
18 T. Xiu, L. Liu, S. Liu, et al., Complexation and extraction of trivalent actinides over lanthanides using highly soluble phenanthroline diamide ligands with different side chains. *J. Hazard. Mater.* **465**, 133508 (2024).
19 F.W. Lewis, L.M. Harwood, M.J. Hudson, et al., Highly efficient separation of actinides from lanthanides by a

phenanthroline-derived bis-triazine ligand. *J. Am. Chem. Soc.* **133**(33), 13093–13102 (2011).
20 S.A. Labb, K.N. Kmak, J.D. Despotopulos, et al., Group hexavalent actinide separation from lanthanides using sodium bismuthate chromatography. *J. Chromatogr. A* **1736**, 465400 (2024).
21 X. Yang, D. Fang, L. Chen, et al., Computation-aided development of next-generation extractants for trivalent actinide and lanthanide separation. *JACS Au* **4**(12), 4744–4756 (2024).
22 N.P. Bessen, I.A. Popov, C.R. Heathman, et al., Complexation of lanthanides and heavy actinides with aqueous sulfur-donating ligands. *Inorg. Chem.* **60**(9), 6125–6134 (2021).
23 J. Liu, Y. Tian, S. Yang, et al., Analysis of explosion incidents in nuclear fuel reprocessing facilities and recommendations for their prevention. *Int. J. Adv. Nucl. Reactor Des. Technol.* **6**(2), 108–116 (2024).
24 J. Liu, S. Yang, Q. Li, et al., Machine learning for forecasting factory concentrations of nitrogen oxides from univariate data exploiting trend attributes. *Int. J. Adv. Nucl. Reactor Des. Technol.* **6**(2), 117–122 (2024).
25 L.S. Fletcher, N.A. Joyner, E.A. Agyei, et al., Non-c2-symmetric complexant for minor actinide separation of actinides from lanthanides. *Chem. Eur. J.* e202500016 (2025).
26 D. Shi, B. Cui, L. Li, et al., Removal of calcium and magnesium from lithium concentrated solution by solvent extraction method using D2EHPA. *Desalination* **479**, 114306 (2020).
27 Y. Dai, Y. Li, W. Hu, et al., Functionalized ionic liquids based on DODGA with enhanced Eu(III)/U(VI) separation efficiency in highly acidic environment. *J. Mol. Liq.* **387**, 122557 (2023).
28 Y. Cai, Q. Yan, M. Wang, et al., Endowing 2,6-bis-triazolyl-pyridine of poor extraction with superior efficiency for actinide/lanthanide separation at high acidity by anchoring to a macrocyclic scaffold. *J. Hazard. Mater.* **416**, 125745 (2021).
29 A. Leoncini, J. Huskens, W. Verboom, Ligands for f-element extraction used in the nuclear fuel cycle. *Chem. Soc. Rev.* **46**(23), 7229–7273 (2017).
30 J. Veliscek-Carolan, Separation of actinides from spent nuclear fuel: A review. *J. Hazard. Mater.* **318**, 266–281 (2016).
31 M.J. Hudson, L.M. Harwood, D.M. Laventine, et al., Use of soft heterocyclic n-donor ligands to separate actinides and lanthanides. *Inorg. Chem.* **52**(7), 3414–3428 (2013).
32 K.L. Nash, The chemistry of TALSPEAK: A review of the science. *Solvent Extr. Ion Exch.* **33**(1), 1–55 (2014).
33 J.C. Braley, T.S. Grimes, K.L. Nash, Alternatives to HDEHP and DTPA for simplified TALSPEAK separations. *Ind. Eng. Chem. Res.* **51**(2), 629–638 (2011).
34 A. Geist, U. Müllich, D. Magnusson, et al., Actinide(III)/lanthanide(III) separation via selective aqueous complexation of Actinides(III) using a hydrophilic 2,6-bis(1,2,4-triazin-3-yl)-pyridine in nitric acid. *Solvent Extr. Ion Exch.* **30**(5), 433–444 (2012).
35 M. Miguirditchian, V. Vanel, C. Marie, et al., Americium recovery from highly active PUREX raffinate by solvent extraction: The EXAm process. *Solvent Extr. Ion Exch.* **38**(4), 365–387 (2020).
36 E.P. Horwitz, W.W. Schulz, in *New Separation Chemistry Techniques for Radioactive Waste and Other Specific Applications* (Eds.: M. L. Cecille, M. Casarci, L. Pietrelli), Springer Dordrecht, Netherlands, pp. 21–29 (1991).
37 X. Jing, J. Wang, H. Cao, et al., Extraction of V(V) and Cr(VI) from aqueous solution using primary amine extractants: Extraction mechanism and oxidation of extractants. *Chem. Pap.* **72**(1), 109–118 (2018).
38 A. Wojciechowska, K. Wieszczycka, I. Wojciechowska, et al., Lead(II) extraction from aqueous solutions by pyridine extractants. *Sep. Purif. Technol.* **177**, 239–248 (2017).
39 V. Vermaak, H.M. Krieg, L. De Beer, et al., Mechanistic study of hafnium and zirconium extraction with organophosphorus extractants. *Solvent Extr. Ion Exch.* **36**(2), 150–161 (2018).
40 Y. Lu, H. Wei, Z. Zhang, et al., Selective extraction and separation of thorium from rare earths by a phosphorodiamidate extractant. *Hydrometallurgy.* **163**, 192–197 (2016).
41 Z. Peng, D. Linfei, Z. Dongxiang, et al., Efficient extraction of Nd (III) by calix[4]arene derivatives containing diethyl phosphite. *Hydrometallurgy.* **169**, 47–58 (2017).
42 N.P. Bessen, J.A. Jackson, M.P. Jensen, et al., Sulfur donating extractants for the separation of trivalent actinides and lanthanides. *Coord. Chem. Rev.* **421**, 213446 (2020).
43 J.E. Birkett, M.J. Carrott, O.D. Fox, et al., Recent developments in the purex process for nuclear fuel reprocessing: Complexant based stripping for uranium/plutonium separation. *Chimia.* **59**(12), 898–904 (2005).
44 A. Wilden, G.J. Lumetta, F. Sadowski, et al., An advanced TALSPEAK concept for separating minor actinides. Part 2. Flowsheet test with actinide-spiked simulant. *Solvent Extr. Ion Exch.* **35**(6), 396–407 (2017).
45 G.R. Choppin, Studies of the synergistic effect. *Sep. Sci. Technol.* **16**(9), 1113–1126 (1981).
46 A.E. Clark, P. Yang, J.C. Shafer, *Coordination of actinides and the chemistry behind solvent extraction*, J.K. Gibson, W.A. de Jong (Eds.), In *Experimental Theorectical to Approaches Actinide Chem.* John Wiley & Sons, 237–282 (2018). https://doi.org/10.1002/9781119115557.ch5
47 K. Matloka, A.K. Sah, P. Srinivasan, et al., Design, synthesis and evaluation of carbamoylmethylphosphine sulfide (CMPS)-based chelates for separation of lanthanides and actinides. *Compt. Rendus Chim.* **10**(10–11), 1026–1033 (2007).
48 V.Y. Aleksenko, E.V. Sharova, O.I. Artyushin, et al., Coordination of p(x)-modified (x=o, s) n-aryl-carbamoylmethylphosphine oxides and sulfides with Pd(II) and Re(I) ions: Facile formation of 6,6-membered pincer complexes featuring atropisomerism. *Polyhedron.* **51**, 168–179 (2013).
49 Q. Xu, J. Wu, Y. Chang, et al., Extraction of Am(III) and Lanthanides(III) with organo dithiophosphinic acids. *Radiochim. Acta.* **96**(12), 771–779 (2008).
50 J.L. Lefferts, K.C. Molloy, J.J. Zuckerman, et al., Oxy and thio phosphorus acid derivatives of tin. 1. Triorganotin(IV) dithiophosphate esters. *Inorg. Chem.* **19**(6), 1662–1670 (1980).
51 D. Pattee, C. Musikas, A. Faure, et al., Extraction des lanthanides et actinides trivalents par l'acide di-2-ethylhexyldithiophosphorique: Structure des complexes organiques. *JLCM.* **122**, 295–302 (1986).
52 R. Takayama, K. Ooe, W. Yahagi, et al., Solvent extraction of trivalent actinides with di(2-ethylhexyl) phosphoric acid. *Proc. Radiochem.* **1**(1), 157–160 (2011).
53 M.P. Jensen, A.H. Bond, Comparison of covalency in the complexes of trivalent actinide and lanthanide cations. *J. Am. Chem. Soc.* **124**(33), 9870–9877 (2002).

54 A. Bhattacharyya, P. Mohapatra, V. Manchanda, Separation of Americium(III) and Europium(III) from nitrate medium using a binary mixture of cyanex-301 with n-donor ligands. *Solvent Extr. Ion Exch.* **24**, 1–17 (2006).

55 D. Wyrzykowski, J. Pranczk, D. Jacewicz, et al., Investigations of ternary complexes of Co(II) and Ni(II) with thiodiacetate anion and 1,10-phenanthroline or 2,2′-bipyridine in aqueous solutions. *Open Chem.* **13**(1), 369–375 (2015).

56 A. Geist, P.J. Panak, Recent progress in trivalent actinide and lanthanide solvent extraction and coordination chemistry with triazinylpyridine N donor ligands. *Solvent Extr. Ion Exch.* **39**(2), 128–151 (2021).

57 M.V. Evsiunina, P.I. Matveev, S.N. Kalmykov, et al., Solvent extraction systems for separation of an(III) and ln (III): Overview of static and dynamic tests. *Mosc. Univ. Chem. Bull.* **76**(5), 287–315 (2021).

58 C. Hill, C. Madic, P. Baron, et al., Trivalent minor actinides/lanthanides separation, using organophosphinic acids. *J. Alloy. Compd.* **271**, 159–162 (1998).

59 X. Yang, S. Wang, L. Xu, et al., New tetradentaten, o-hybrid phenanthroline-derived organophosphorus extractants for the separation and complexation of trivalent actinides and lanthanides. *Inorg. Chem. Front.* **9**(18), 4671–4684 (2022).

60 I. Goldberg, D. Meyerstein, Influence of ion exchanger and diluent structure on uranyl ion selective electrode response. *Anal. Chem.* **52**(13), 2105–2108 (1980).

61 S. Deng, D. Shuai, Q. Yu, et al., Selective sorption of perfluorooctane sulfonate on molecularly imprinted polymer adsorbents. *Front. Environ. Sci. Eng. China.* **3**(2), 171–177 (2009).

62 Z. Kolarik, Complexation and separation of lanthanides(III) and actinides(III) by heterocyclic n-donors in solutions. *Chem. Rev.* **108**(10), 4208–4252 (2008).

63 X. Zhang, Q. Wu, J. Lan, et al., Highly selective extraction of pu (IV) and am (III) by N,N′-diethyl-N,N′-ditolyl-2,9-diamide-1,10-phenanthroline ligand: An experimental and theoretical study. *Sep. Purif. Technol.* **223**, 274–281 (2019).

64 P. Wei, N. Pu, X. Dong, et al., Structural and stability trends of the complexation of hexavalent actinides with two dipicolinic acid derivatives: An experimental and theoretical study. *Inorg. Chem.* **58**(17), 11664–11671 (2019).

65 H. Wang, P. Gao, T. Cui, et al., New asymmetric tetradentate phenanthroline chelators with pyrazole and amide groups for complexation and solvent extraction of Ln (III)/Am(III). *Dalton Trans.* **53**(2), 601–611 (2024).

66 S. Wang, J. Lou, X. Yang, et al., Unsymmetrical amide-lactam-phenanthroline (ALPhen) extractant for selective separation of actinides and lanthanides. *Ind. Eng. Chem. Res.* **64**(38), 15830–15840 (2025).

67 M. Galletta, L. Baldini, F. Sansone, et al., Calix [6] arene-picolinamide extractants for radioactive waste: Effect of modification of the basicity of the pyridine n atom on the extraction efficiency and an/ln separation. *Dalton Trans.* **39**(10), 2546 (2010).

68 L. Nigond, N. Condamines, P.Y. Cordier, et al., Recent advances in the treatment of nuclear wastes by the use of diamide and picolinamide extractants. *Sep. Sci. Technol.* **30**(7–9), 2075–2099 (1995).

69 F. Gao, X. Xu, X. Yang, et al., Completely preorganized bis-lactam-1,10-phenanthroline ligands with high stability for efficient separation of Am(III) over Eu(III). *Dalton Trans.* **54**(7), 2871–2876 (2025).

70 A.M. Safiulina, E.I. Goryunov, A.A. Letyushov, et al., Effect of anomalous aryl strengthening in the series of N-phosphorylureas. *Mendeleev Commun.* **19**(5), 263–265 (2009).

71 I. Uson, G.M. Sheldrick, An introduction to experimental phasing of macromolecules illustrated by SHELX; New autotracing features. *Acta Crystallogr. D.* **74**(2), 106–116 (2018).

72 B.J. Mincher, C.M. Wai, R.V. Fox, et al., The separation of lanthanides and actinides in supercritical fluid carbon dioxide. *J. Radioanal. Nucl. Chem.* **307**(3), 2543–2547 (2016).

73 S.S. Koegler, Development of a unique process for recovery of uranium from incinerator ash. *Nuclear Energy Environment*, **1046**, 65–78 (2010).

74 D.L. Quach, B.J. Mincher, C.M. Wai, Supercritical fluid extraction and separation of uranium from other actinides. *J. Hazard. Mater.* **274**, 360–366 (2014).

75 M. Zhou, Z. Liu, Z. Dai, et al., Efficient separation of Pr(III) and Nd(III) via shear-induced dissociation coupling with ultrafiltration: Insights from experiments and theory. *Ind. Eng. Chem. Res.* **64**(1), 740–751 (2024).

76 Q. Wu, F. Zhang, Q. Huang, et al., A novel one-step strategy for extraction and solidification of Th(IV) based on self-assembly driven by malonamide-based $[DC18DMA]^+$ ionic liquids. *Chem. Eng. J.* **430**, 132717 (2022).

77 P. Zsabka, A. Wilden, K. Van Hecke, et al., Beyond U/Pu separation: Separation of americium from the highly active PUREX raffinate. *J. Nucl. Mater.* **581**, 154445 (2023).

78 Z. Wang, K. Zhang, G. Chen, et al., Evolutionary-assisted reinforcement learning for reservoir real-time production optimization under uncertainty. *Pet. Sci.* **20**(1), 261–276 (2023).

79 Z. Wang, L. Huang, X. Dong, et al., Ion sieving in graphene oxide membrane enables efficient actinides/lanthanides separation. *Nat. Commun.* **14**(1), 261 (2023).

80 J.G.O. Connell-Danes, B.T. Ngwenya, C.A. Morrison, et al., Selective separation of light rare-earth elements by supramolecular encapsulation and precipitation. *Nat. Commun.* **13**(1), 4497 (2022).

81 T.P. Gompa, A. Ramanathan, N.T. Rice, et al., The chemical and physical properties of tetravalent lanthanides: Pr, Nd, Tb, and Dy. *Dalton Trans.* **49**(45), 15945–15987 (2020).

82 C. Stetson, D. Prodius, H. Lee, et al., Solvent-driven fractional crystallization for atom-efficient separation of metal salts from permanent magnet leachates. *Nat. Commun.* **13**(1), 3789 (2022).

83 X. Yin, Y. Wang, X. Bai, et al., Rare earth separations by selective borate crystallization. *Nat. Commun.* **8**, 14438 (2017).

84 T. Kikuchi, T. Koyama, S. Homma, Development of reprocessing process by plutonium cocrystallization. *AIP Conf. Proc.* **673**(1), 42–44 (2003).

85 X. Yin, Y. Wang, X. Li, et al., Competing crystallization between lanthanide and actinide in acidic solution leading to their efficient separation. *Chin. J. Chem.* **37**(1), 53–57 (2019).

86 Y. Li, H. Lu, Y. Du, et al., Highly efficient separation of high-valent actinide ions from lanthanides via fractional crystallization. *Chin. J. Struct. Chem.* **44**(4), 100562 (2025).

87 H. Zhang, A. Li, K. Li, et al., Ultrafiltration separation of Am(VI)-polyoxometalate from lanthanides. *Nature.* **616**(7957), 482–487 (2023).

88 Q.Y. Zhang, L.J. Zhang, J.Q. Zhu, et al., Ultra-selective uranium separation by in-situ formation of π-f conjugated 2d uranium-organic framework. *Nat. Commun.* **15**(1), 453 (2024).

89 X. Zhao, M. Wong, C. Mao, et al., Size-selective crystallization of homochiral camphorate metal–organic frameworks for lanthanide separation. *J. Am. Chem. Soc.* **136**(36), 12572–12575 (2014).

90 M. Keener, C. Hunt, T.G. Carroll, et al., Redox-switchable carboranes for uranium capture and release. *Nature.* **577**(7792), 652–655 (2020).

91 S.A. Ansari, P.K. Mohapatra, A review on solid phase extraction of actinides and lanthanides with amide based extractants. *J. Chromatogr. A.* **1499**, 1–20 (2017).

92 R.B. Gujar, P.K. Mohapatra, D.S. Lakshmi, et al., Composite polymeric beads containing N, N, N′, N′-tetraoctyldiglycolamide for actinide ion uptake from nitric acid feeds: Batch uptake, kinetic modelling and column studies. *J. Chromatogr. A.* **1422**, 206–212 (2015).

93 J.A. Mattocks, J.A. Cotruvo, Biological, biomolecular, and bio-inspired strategies for detection, extraction, and separations of lanthanides and actinides. *Chem. Soc. Rev.* **49**(22), 8315–8334 (2020).

94 T. Yuan, S. Xiong, X. Shen, Coordination of actinide single ions to deformed graphdiyne: Strategy on essential separation processes in nuclear fuel cycle. *Angew. Chem. Int. Ed.* **59**(40), 17719–17725 (2020).

95 Z. Huang, Z. Li, Q. Wu, et al., Simultaneous elimination of cationic uranium(VI) and anionic rhenium(VII) by graphene oxide-poly(ethyleneimine) macrostructures: A batch, XPS, EXAFS, and DFT combined study. *Environ. Sci. Nano.* **5**(9), 2077–2087 (2018).

96 D. Shao, G. Hou, J. Li, et al., PANI/GO as a super adsorbent for the selective adsorption of uranium(VI). *Chem. Eng. J.* **255**, 604–612 (2014).

97 K. Goh, H.E. Karahan, L. Wei, et al., Carbon nanomaterials for advancing separation membranes: A strategic perspective. *Carbon.* **109**, 694–710 (2016).

98 L. Chen, G. Shi, J. Shen, et al., Ion sieving in graphene oxide membranes via cationic control of interlayer spacing. *Nature.* **550**(7676), 380–383 (2017).

99 R.K. Joshi, P. Carbone, F.C. Wang, et al., Precise and ultrafast molecular sieving through graphene oxide membranes. *Science.* **343**(6172), 752–754 (2014).

100 R.K. Joshi, S. Alwarappan, M. Yoshimura, et al., Graphene oxide: The new membrane material. *Appl. Mater. Today.* **1**(1), 1–12 (2015).

101 P. Gouzerh, A. Proust, Main-group element, organic, and organometallic derivatives of polyoxometalates. *Chem. Rev.* **98**(1), 77–112 (1998).

102 R. Copping, C. Talbot-Eeckelaers, D. Collison, et al., Probing the 5f electrons in a plutonyl(VI) cluster complex. *Dalton Trans.* **7**(29), 5609 (2009).

103 M. Sepesy, B. Fugate, C.E. Duval, Amine-functionalized membrane adsorbers to purify copper from acidic solutions. *ACS Appl. Polym. Mater.* **4**(5), 3034–3044 (2022).

104 M. Wu, J. Yan, T. Ji, et al., Synthesis of (222)-oriented defect-rich MOF-808 membranes towards high-efficiency uranium rejection. *J. Membr. Sci.* **717**, 123570 (2025).

105 W. Dong, J. Yan, T. Ji, et al., Eliminating lattice defects in UiO-66-NH2 membrane towards high-precision desalination. *Adv. Membr.* **5**, 100142 (2025).

106 Y. Zhang, M. Yan, T. Wang, et al., Microstructure optimization of the MIP-177-LT membrane for highly efficient uranium separation from seawater. *Ind. Eng. Chem. Res.* **64**(27), 13826–13833 (2025).

107 Y. Zhang, J. Liu, S. Du, et al., Fabrication of MIP-201 membrane with excellent stability for high-efficiency uranium separation from seawater. *J. Membr. Sci.* 124921 (2025).

108 M.N. Sokolova, A.M. Fedosseev, G.B. Andreev, et al., Synthesis and structural examination of complexes of Am(IV) and other tetravalent actinides with lacunary heteropolyanion α_2-P_2W_{17061}. *Inorg. Chem.* **48**(19), 9185–9190 (2009).

Cite this article as: Zhang Y, Jin X, Wang M, Sun K, Ge M, Noro S-I & Liu Y. Recent progress on the separation of lanthanide/actinide elements from nuclear wastes. **2**, 2026002 (2026), https://doi.org/10.1051/rdne/2026002.